Exploring Potential Connections Between Fast Radio Bursts, Gamma-ray Bursts, and Magnetars

Kaitlyn Parrinello

Istituto Nazionale di Fisica Nucleare – Sezione di Trieste
Università degli Studi di Trieste

WHAT ARE FAST RADIO BURSTS (FRBS)?

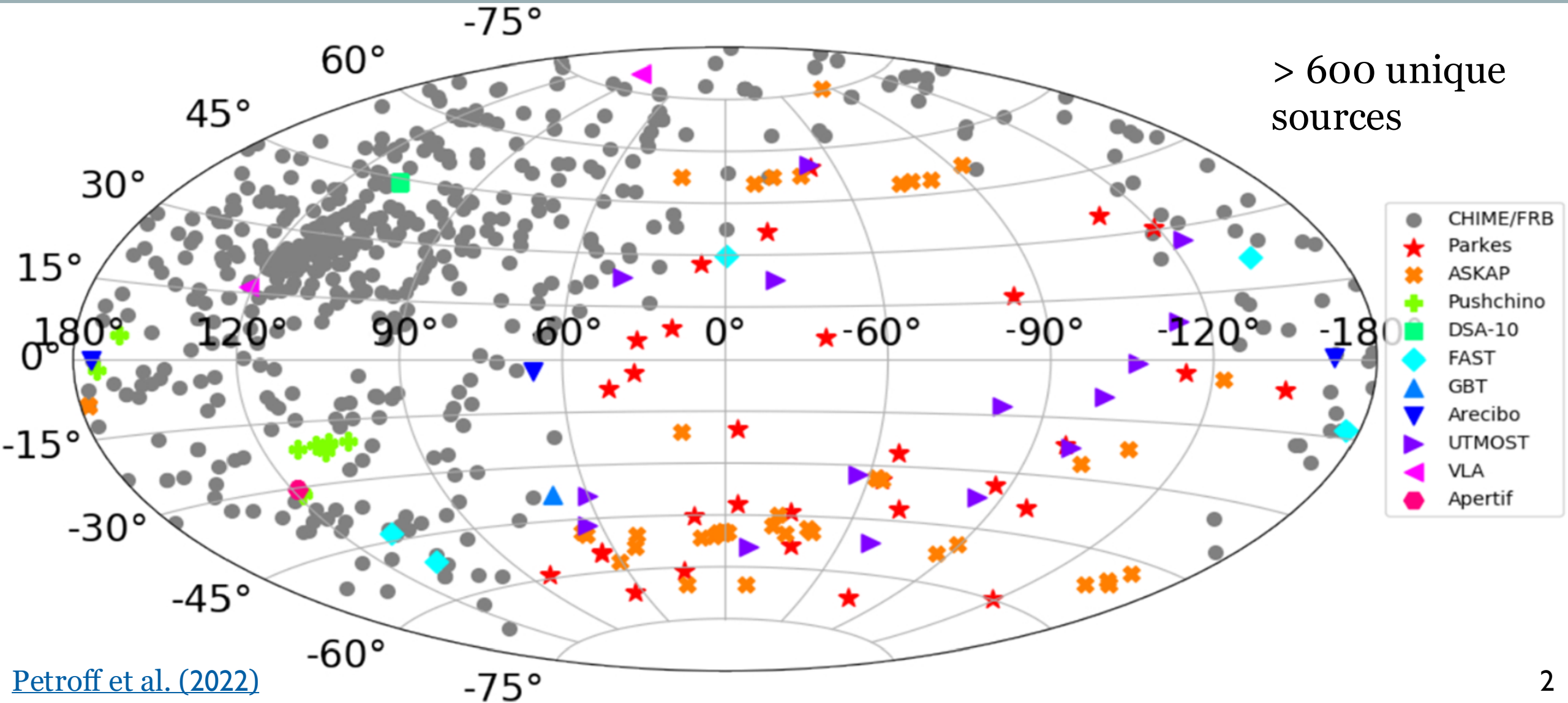

> 600 unique sources

Petroff et al. (2022)

WHAT ARE GAMMA-RAY BURSTS (GRBS)?

- Most luminous events observed
- Short, bright pulses of gamma-rays
- Timescales: a fraction of a second to several hundred seconds
- Cosmological and isotropic

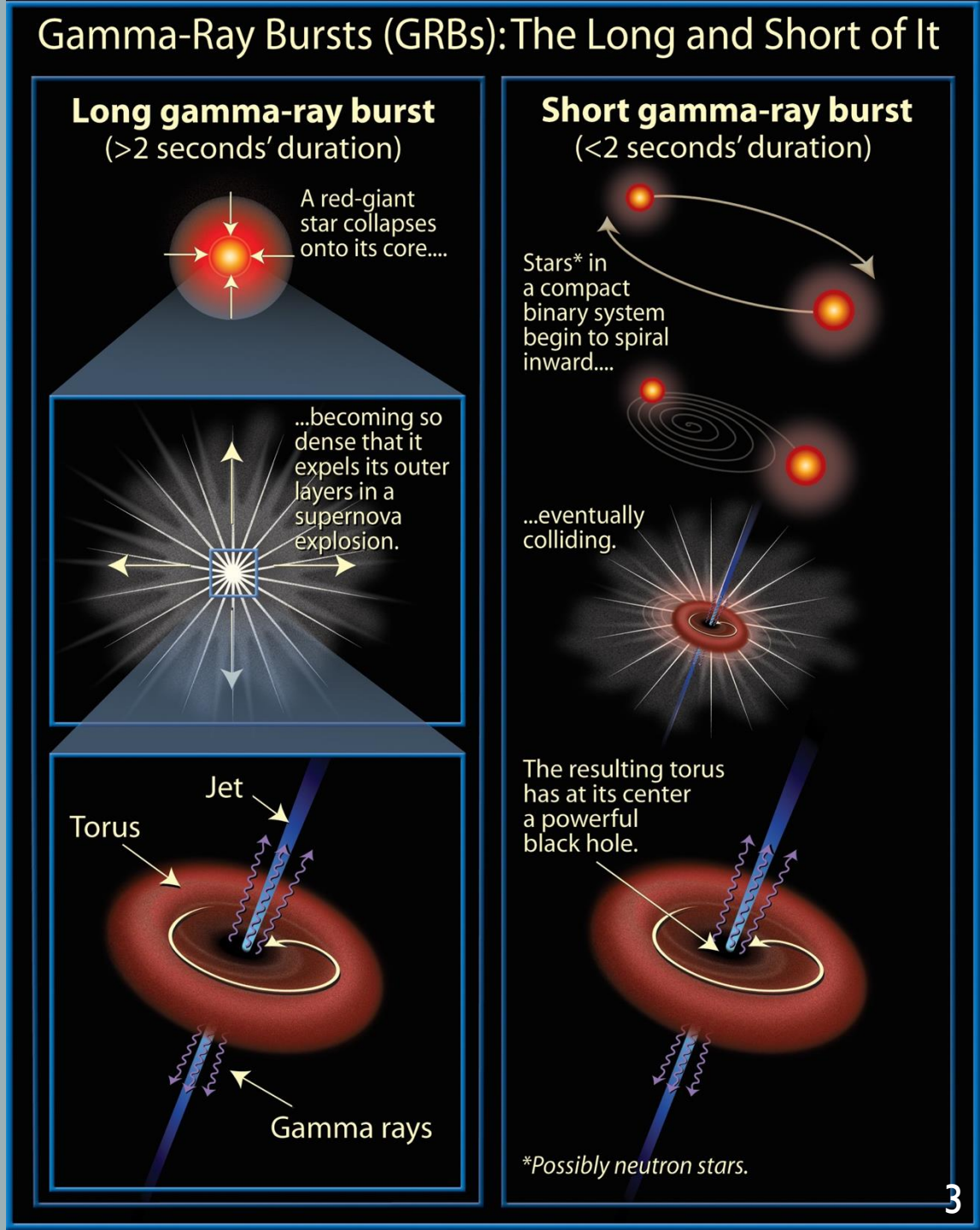

Credit: NASA and A. Feild (STScI)

FRBS & GRBS: LAT ANALYSIS

- Sample size from CHIME/FRB: 589 FRBs [CHIME/FRB Collaboration et al. (2021); Chime/Frb Collaboration et al. (2023)]
  - Non-repeaters = 525
  - Repeaters = 64 (repeat bursts = 469)
- Automatic unbinned likelihood analysis pipeline based on GtBurst code [Vianello, G. (2016)]

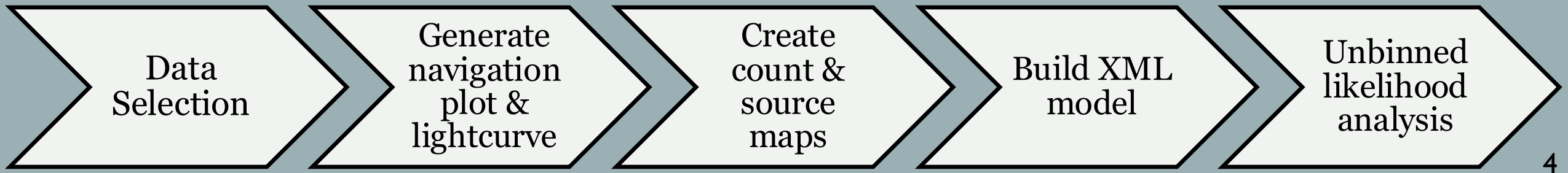

LAT RESULTS

Table 1. CHIME/FRB Non-Repeaters with TS ≥ 5

FRB Name	RA (deg)	Dec (deg)	MJD_400 (MJD)	Trigger time (MET)	TS	Energy Flux ($erg\ cm^{-2}s^{-1}$)	Photon Flux ($ph\ cm^{-2}s^{-1}$)
FRB20181228C	265.19	54.36	58480.803015	567717385.461	8	1.94×10^{-8}	4.73×10^{-5}
FRB20190422B	158.27	45.67	58595.187933	577600242.449	5	4.02×10^{-9}	9.8×10^{-6}
FRB20190601C	88.52	28.47	58635.884481	581116424.192	6	9.23×10^{-8}	2.25×10^{-4}
FRB20190623B	335.22	46.12	58657.511784	582985023.143	8	3.57×10^{-9}	8.71×10^{-6}
FRB20190624A	168.32	69.78	58658.048374	583031384.481	11	8.27×10^{-9}	2.02×10^{-5}

Table 2. CHIME/FRB Repeaters with TS ≥ 5

FRB Name	FRB Burst Name	RA (deg)	Dec (deg)	MJD_400 (MJD)	Trigger time (MET)	TS	Energy Flux ($erg\ cm^{-2}s^{-1}$)	Photon Flux ($ph\ cm^{-2}s^{-1}$)
FRB20200104D	FRB20180916B	188.21387	74.1512	58852.137732	599800705.06	5	1.29×10^{-8}	3.14×10^{-5}
FRB20220321C	FRB20181119A	190.44426	65.1242	59659.362586	669544932.41	11	6.71×10^{-9}	1.64×10^{-5}
FRB20190116A	FRB20190116A	192.27384	27.1405	58499.546921	569336858.945	5	7.92×10^{-9}	1.93×10^{-5}
FRB20211125A	FRB20190303A	207.99999	48.1220	59543.732553	659554497.565	5	5.11×10^{-9}	1.25×10^{-5}
FRB20210331B	FRB20201124A	77.01426	26.0607	59304.026793	638843919.938	5	9.98×10^{-9}	2.43×10^{-5}

POSITION-HISTORY DATA: FRB20181228C

gdt-core
The Gamma-ray Data Tools Core Package

Goldstein et al. (2024)

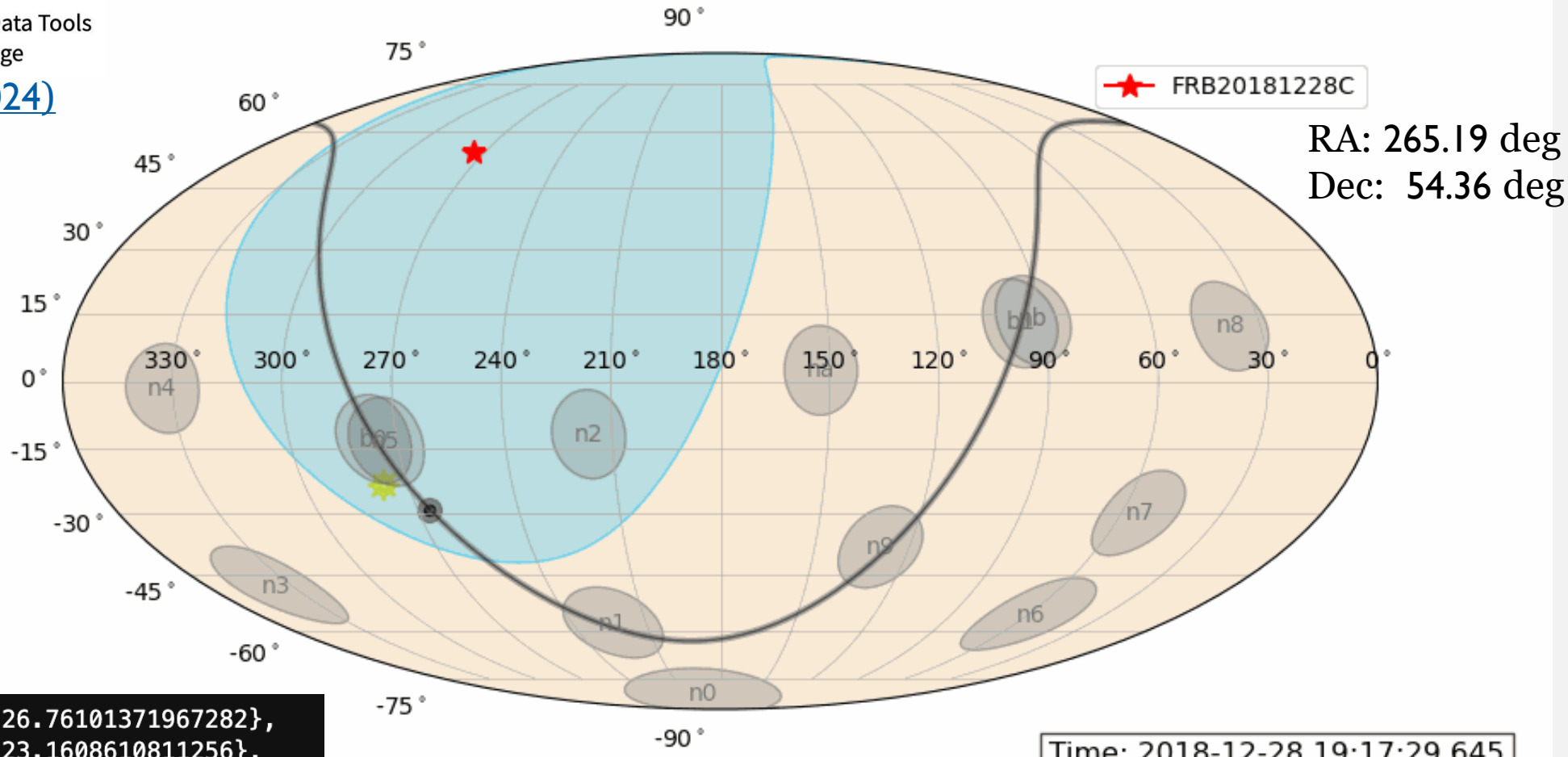

RA: 265.19 deg
Dec: 54.36 deg


```
{'TT_frame_14': {'n2': 26.76101371967282},
 'TT_frame_15': {'n2': 23.1608610811256},
 'TT_frame_16': {'n2': 19.997750933576935},
 'TT_frame_17': {'n2': 18.12579153119106},
 'TT_frame_18': {'n2': 23.543712795473112},
 'TT_frame_19': {'n1': 29.512535175595723}}
```

TIME TAGGED EVENT DATA: FRB20181228C

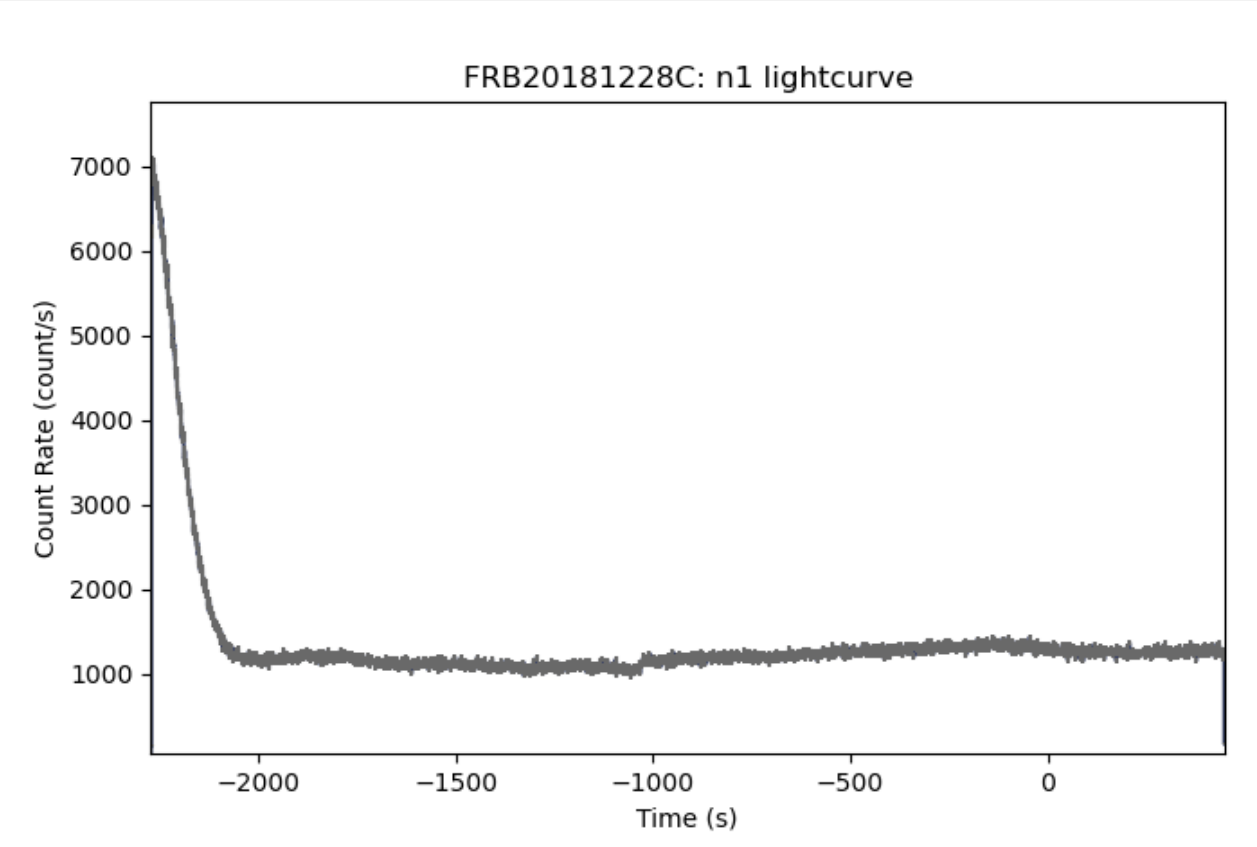

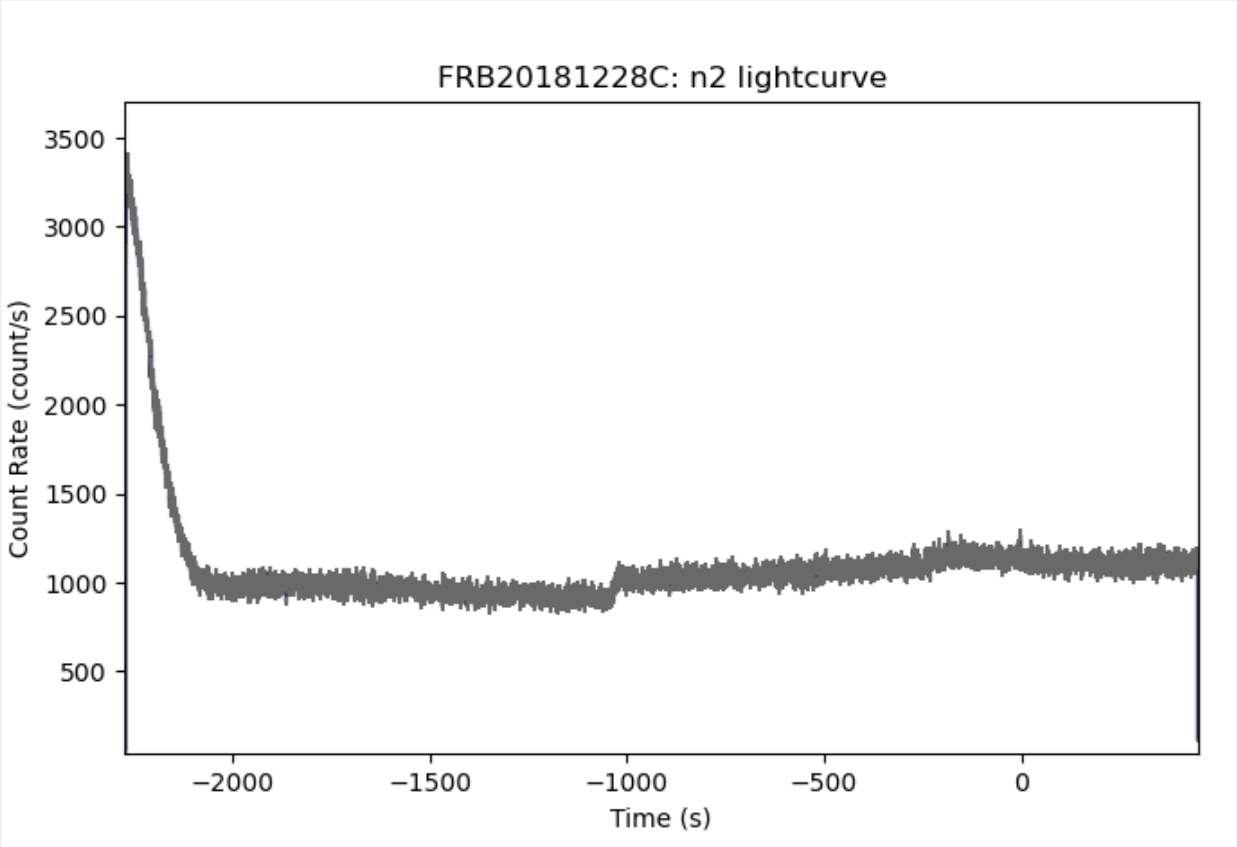

SGR 1935+2154

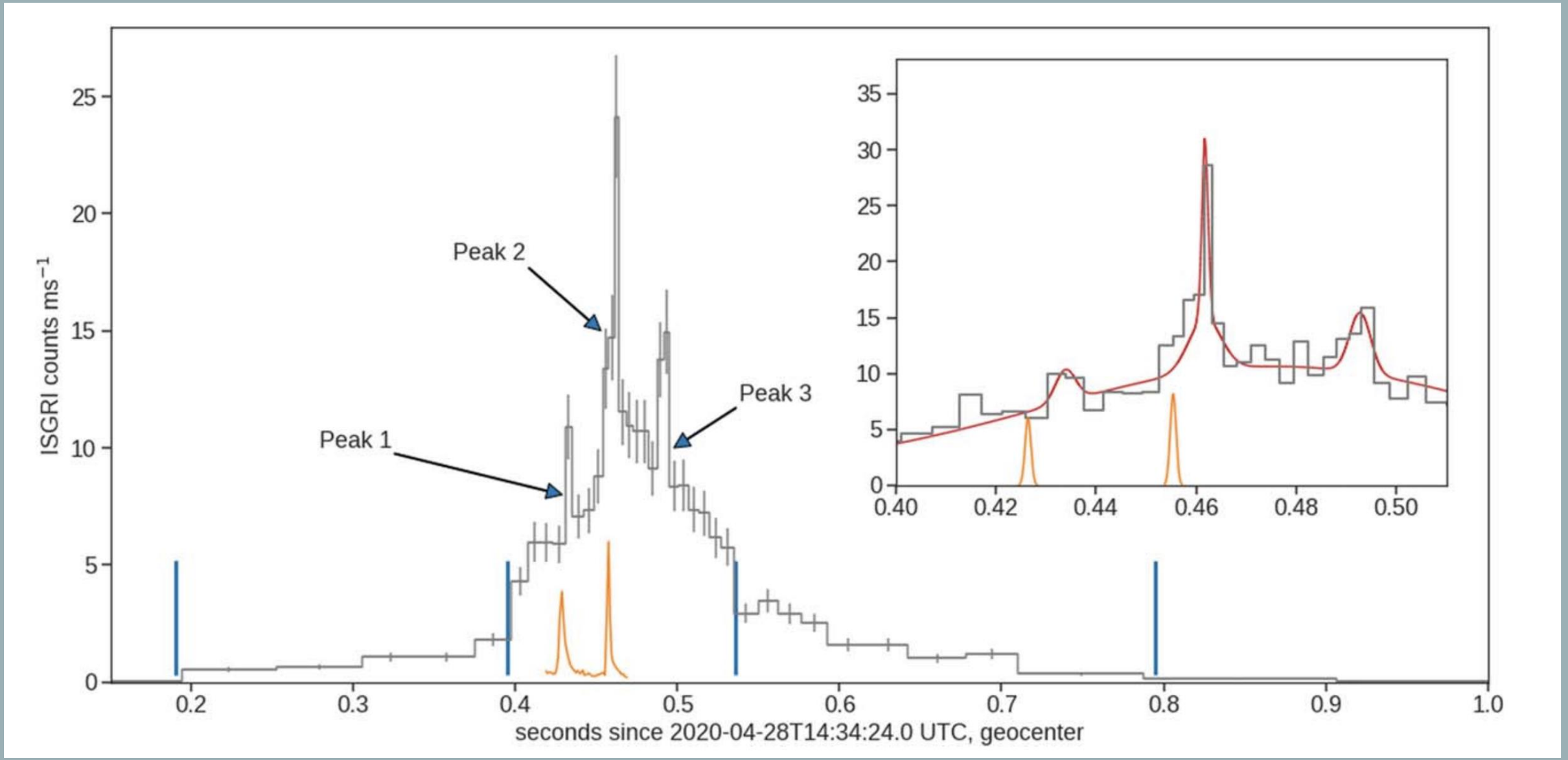

Mereghetti et al. 2020

MAGNETAR, SGR, AND REPEATER FRB RELATION?

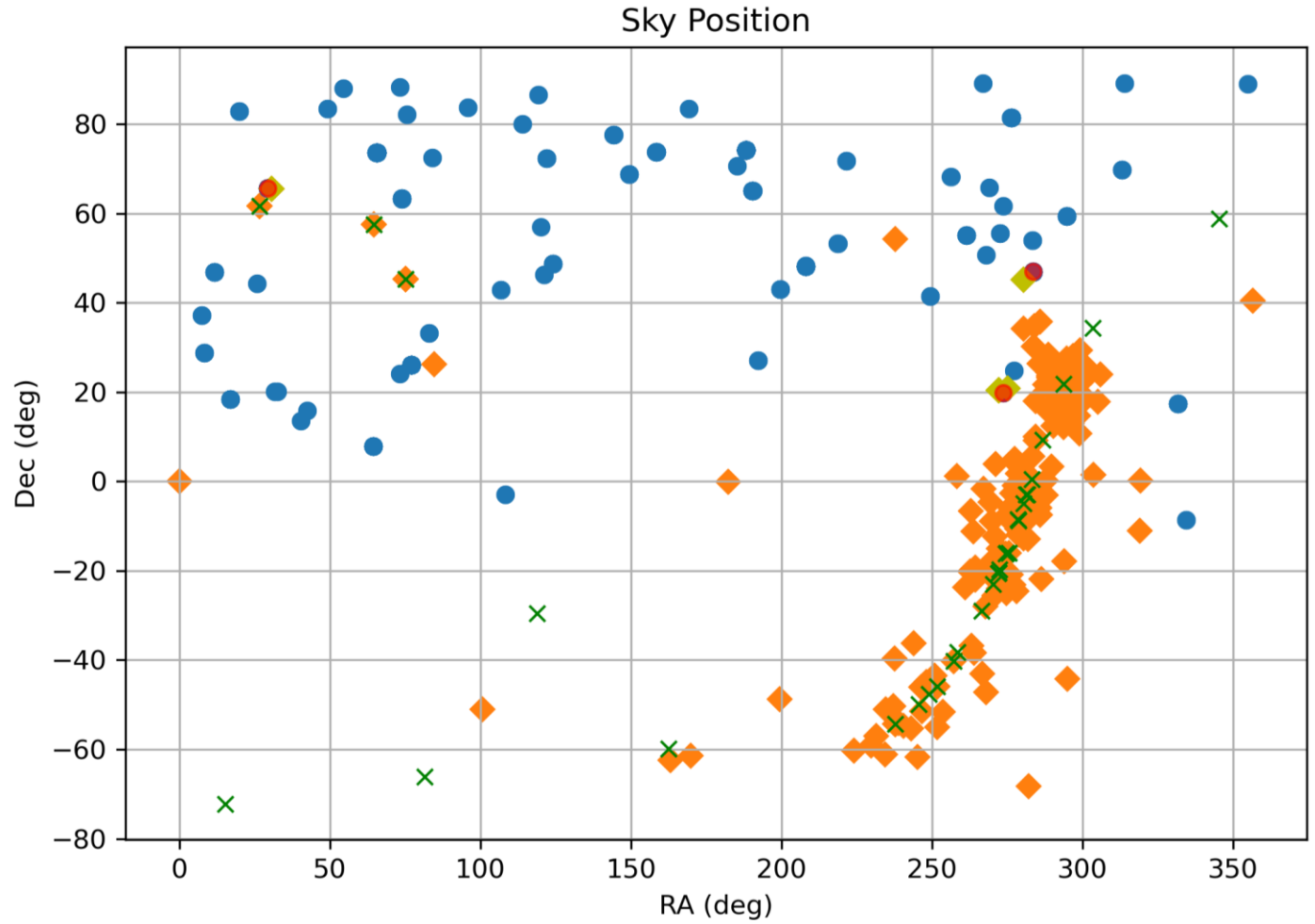

Chime/Frb Collaboration et al. (2023)
Olausen & Kaspi (2014)
http://www.physics.mcgill.ca/~pulsar/magnetar/main.html
von Kienlin et al. (2020)

SUMMARY

- LAT & GBM Analysis:
  - No coinciding FRBs and GRBs
  - Calculated upper limits on photon and energy flux
- Repeater FRBs, Magnetars, SGRs:
  - Confirmed FRB with SGR 1935+2154
  - My search: Spatially related, not temporally

THANK YOU!

BACKUP SLIDES

DATA SELECTION

- Astroquery Fermi-LAT server
- RA, Dec of FRB
- Trigger time = MJD_400 → UTC → MET
- TSTART = trigtime – 5000;
- TSTOP = trigtime + 20000
- Searchradius = 60
- energyrange_MeV = 30,1000000
- LATdatatype = Extended

NAVIGATION PLOT

- Zenith angle: Angle w.r.t Earth's limb
- Source off-axis angle: Angle between source and detector

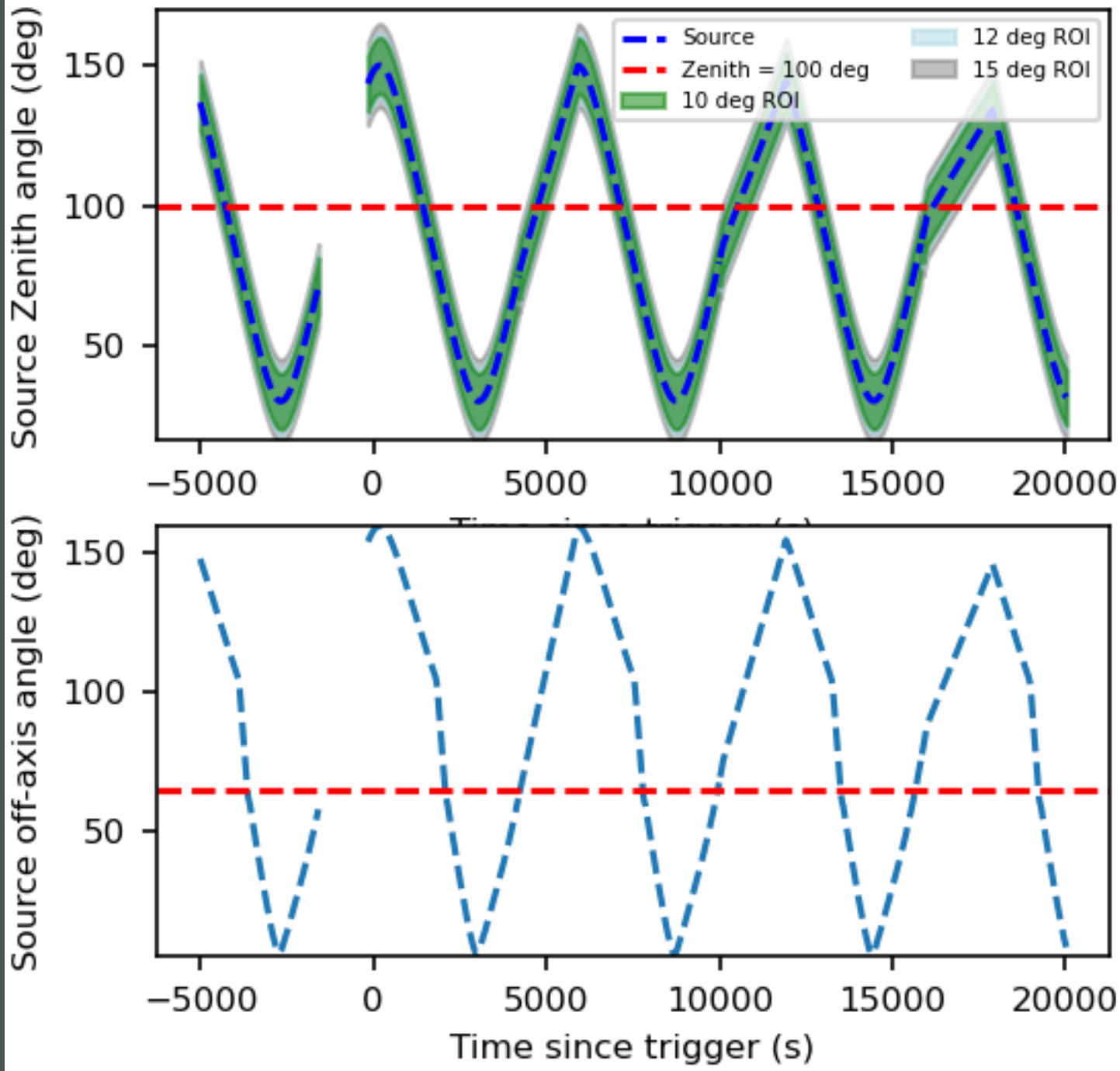

SOURCE MAP

- Rad = 12
- IRF = p8_transient020e
- Zmax=100
- Emin = 100
- Emax = 100000
- Tstart, tstop = ranges of 100s
  - Starting 0-100

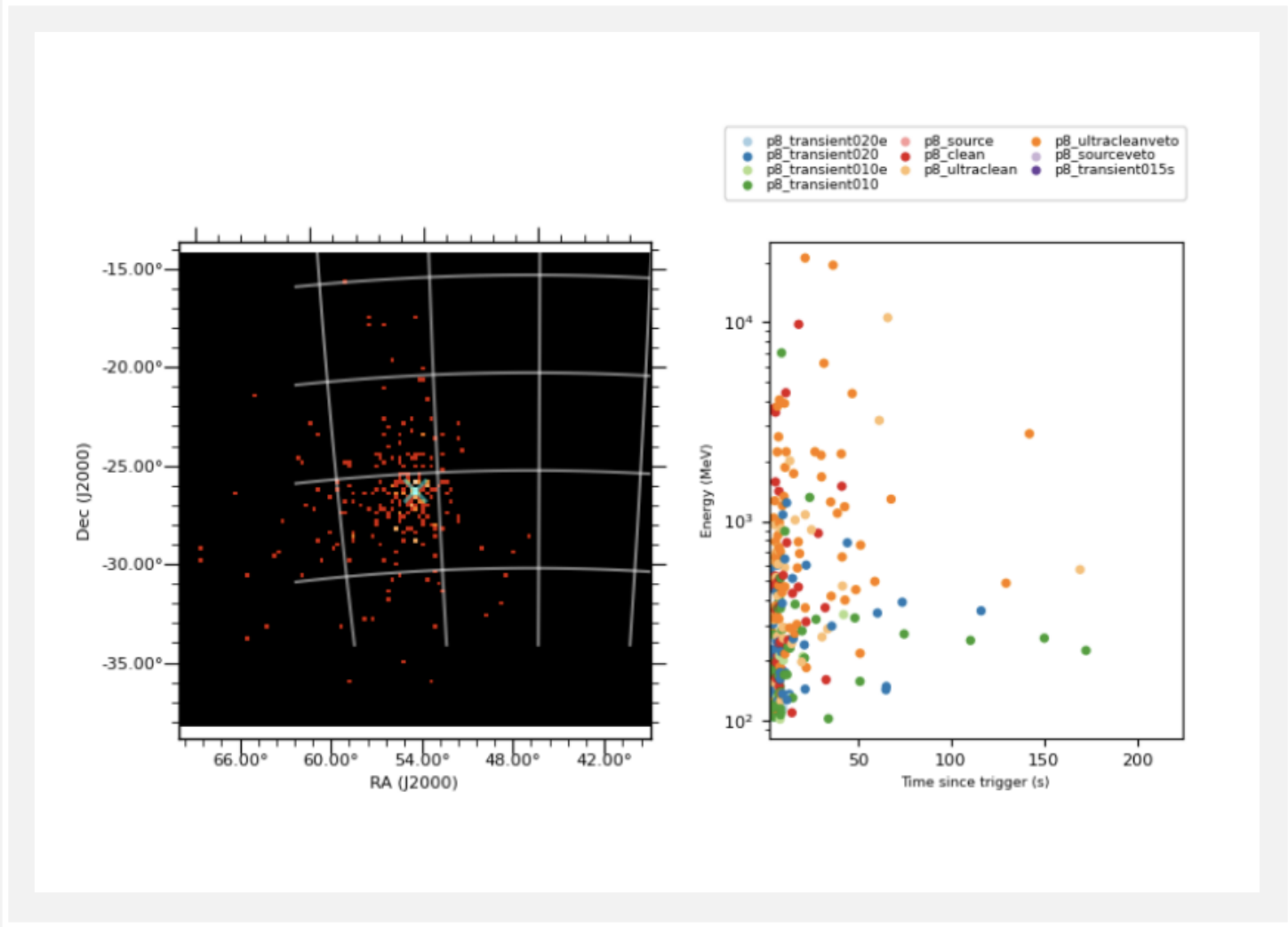

Source Name	Name	Value	Error	Min	Max	Scale	Free	Source Type	Feature	Feature Type	Feature Fi
bn190114873	Integral	0.01		1e-05	1000.0	0.001	1	PointSource	spectrum	PowerLaw2	
bn190114873	Index	-2		-6.0	0.01	1.0	1	PointSource	spectrum	PowerLaw2	
bn190114873	LowerLimit	100		20.0	200000.	1.0	0	PointSource	spectrum	PowerLaw2	
bn190114873	UpperLimit	1e+05		20.0	500000	1.0	0	PointSource	spectrum	PowerLaw2	
bn190114873	RA	54.5		-360.	360.0	1.0	0	PointSource	spatialMode	SkyDirFunction	
bn190114873	DEC	-26.9		-90.0	90.0	1.0	0	PointSource	spatialMode	SkyDirFunction	
IsotropicTemplate	Normalizatio	1		0.1	10.0	1	1	DiffuseSourc	spectrum	FileFunction	[..]/iso_P8R3_TRANSIEI
IsotropicTemplate	Value	1		0.0	10.0	1.0	0	DiffuseSourc	spatialMode	ConstantValue	
GalacticTemplate	Value	1		0.7	1.3	1.0	0	DiffuseSourc	spectrum	ConstantValue	
GalacticTemplate	Normalizatio	1		0.001	1000.0	1.0	0	DiffuseSourc	spatialMode	MapCubeFunctio	[..]/gll_iem_v07_cut.fits

XML MODEL

- In my case, the model is fixed to the default options
- Fits a power law:

$$\frac{dN}{dE} = \frac{N(\gamma+1)E^{\gamma}}{E_{\max}^{\gamma+1} - E_{\min}^{\gamma+1}}$$

- Integral = N
- Index = γ
- LowerLimit = $E_{\min}$
- UpperLimit = $E_{\max}$

https://fermi.gsfc.nasa.gov/ssc/data/analysis/scitools/source_models.html

LIKELIHOOD ANALYSES

What is it? Likelihood L is the probability of obtaining data given an input model

How used in this case? As an accurate mapping of gamma-ray sky to the list of counts produced by LAT

Binned

- Large # of counts
- Preferred method for GRB analysis
- Prompt burst phase

Unbinned

- Short # of counts
- Preferred method for time series analysis
- Temporally extended emission

https://fermi.gsfc.nasa.gov/ssc/data/analysis/scitools/likelihood_tutorial.html
https://fermi.gsfc.nasa.gov/ssc/data/analysis/documentation/Cicerone/Cicerone_Likelihood/Likelihood_overview.html

TEST STATISTIC

- Computed from Likelihood Analysis
- Large TS = source present
- $\sigma \sim \sqrt{TS}$

$$TS = -2\ln\left(\frac{L_{max,0}}{L_{max,1}}\right)$$

$L_{max,0}$ = max L value for a model w/o additional source

$L_{max,1}$ = max L value for a model w/additional source at specified location

https://fermi.gsfc.nasa.gov/ssc/data/analysis/documentation/Cicerone/Cicerone_Likelihood/Likelihood_overview.html

POSHIST DATA: FRB20181228C

Detector ID #	Azimuth (deg)	Zenith (deg.)
0	45.9	20.6
1	45.1	45.3
2	58.4	90.2
3	314.9	45.2
4	303.2	90.3
5	3.4	89.8
6	224.9	20.4
7	224.6	46.2
8	236.6	90.0
9	135.2	45.6
10	123.7	90.4
11	183.7	90.3

Table 1. NaI detector measured orientations in spacecraft coordinates (see Fig. 4)

https://arxiv.org/pdf/0908.0450
Meegan et al. (2009)

```
[<SpacecraftFrame: 1 frames;
  obstime=[567717385.461]
  obsgeoloc=[(2498680.26041122, 5702631.85365576, -2982156.12038204) m]
  obsgeovel=[(-6941.33895594, 3103.01131512, 120.11983062) m / s]
  quaternion=[(x, y, z, w) [ 0.73593073, -0.66527551, -0.0477529 , -0.11633624]]>,
 <SpacecraftFrame: 1 frames;
  obstime=[567717485.461]
  obsgeoloc=[(1790822.85587068, 5977792.43214944, -2952063.93333735) m]
  obsgeovel=[(-7201.485267, 2394.6051416, 481.02510691) m / s]
  quaternion=[(x, y, z, w) [ 0.74179221, -0.65760696, -0.08008594, -0.10432466]]>,
 <SpacecraftFrame: 1 frames;
  obstime=[567717585.461]
  obsgeoloc=[(1061291.42170961, 6180589.70107155, -2886144.96575192) m]
  obsgeovel=[(-7374.44502357, 1657.18126898, 836.06675185) m / s]
  quaternion=[(x, y, z, w) [ 0.74647743, -0.6498669 , -0.11136234, -0.08968214]]>]
```

```
{'TT_frame_0': {'b0': 68.04982870484942,
  'b1': 111.9501712951506,
  'n0': 140.69714222502932,
  'n1': 117.30577578994438,
  'n2': 77.92987928336979,
  'n3': 118.14682362851461,
  'n4': 78.52836757831206,
  'n5': 68.25662639265596,
  'n6': 164.6628518139096,
  'n7': 147.15155788008715,
  'n8': 102.47803848041538,
  'n9': 146.39116250221963,
  'na': 101.00731067640126,
  'nb': 111.62863044982097},
```

```
 'TT_frame_1': {'b0': 69.9564629740535,
  'b1': 110.0435370259465,
  'n0': 140.73060412940484,
  'n1': 116.700640250392,
  'n2': 75.76120228263285,
  'n3': 121.67033857002072,
  'n4': 82.54302617595553,
  'n5': 69.9375422359286,
  'n6': 168.68588149013195,
  'n7': 149.5425315757079,
  'n8': 104.53592321262491,
  'n9': 142.3834676426049,
  'na': 96.99657871304495,
  'nb': 109.97453763729891},
```

```
 'TT_frame_2': {'b0': 71.60753602136265,
  'b1': 108.39246397863735,
  'n0': 140.073137031359,
  'n1': 115.62008122066233,
  'n2': 73.36821130408428,
  'n3': 124.92285799511461,
  'n4': 86.48129873910621,
  'n5': 71.36069496018327,
  'n6': 172.64726198023843,
  'n7': 151.88989649199289,
  'n8': 106.82242304822543,
  'n9': 138.39869767376837,
  'na': 93.06695074856478,
  'nb': 108.57884041130255},
```